High-Entropy Alloy Nanomaterials for Electrocatalysis and Batteries: Synthesis, Characterization and Applications

Xuhui Wang

School of Chemistry, University of Nottingham, Nottingham, NG7 2RD, United Kingdom

shyxw6@nottingham.ac.uk

Abstract. High-entropy alloys (HEAs), either in nano or porous bulk forms, as both functional and structural materials, have attracted intensive research and emerged as a prominent area of interest within the field of material science since their novel chemical and physical properties. Recently, emerging HEAs have provided immense possibilities for the development of high-efficiency catalysts with exceptional catalytic activity and enhanced durability because of the strengths HEA-NPs possess, for example, the structural stability realized especially under severe catalytic conditions owing to a high-entropy stabilized structure; the identification of optimal catalysts and widely tailorable atom configuration due to a multielement composition space; the arbitrary multielement mixing results in a variety of active sites and significantly beneficial for multistep catalytic reactions. With the decrease in particle size, HEA nanoparticles (HEA-NPs), excellent candidates for compelling heterogeneous catalysis, exhibit even better performance than bulk HEAs because of the surface and quantum confinement effects. Herein, a review of the latest preparation technologies for diverse categories of HEA-NPs and their impressive applications in electrocatalysis and the rechargeable battery is provided, focusing on water splitting, ammonia decomposition, Li-S battery, and Zn-air battery. Furthermore, the current practical challenges and potential directions of HEA-NPs are proposed, which aim to help fabricate more advanced high-entropy nanomaterials for highly efficient chemical conversion.

Keywords: High-entropy alloy, nanoparticle, electrocatalysis, chemical batteries.

1. Introduction

Conventional alloy involves the mixture of one primary metal element and other slight amount elements, which has an extreme limitation of metallic complexity and broad applications. In 2004, the concept of HEAs containing five or more metals was first introduced by Yeh et al. to further boost the properties and varieties of metal alloys [1]. Notably, a higher mixing entropy due to the increased number of elements ($\Delta S_{mix} = Rlnn$) can lead to the decrease of Gibbs free energy ($\Delta G_{mix} = \Delta H_{mix} - T\Delta S_{mix}$) at high temperatures, thereby improving the durability of single-phase solid solution HEA structures. HEAs possess not only novel characteristics, such as the 'cocktail' effect, synergistic effect, sluggish diffusion effect, and lattice distortion effect, which enable HEAs to show significant advantages in various fields, including catalysis, superionic conductivity and energy storage, but also show customizable phase structure and atom configuration owing to the distinctive chemical and physical features, which make the emerging class of multi-component alloys become a promising candidate for advanced catalysts.

Moreover, nanoscale HEAs exhibit significant increases in specific surface areas, resulting in the exposure of a greater quantity of active areas and enhanced utilization efficiency of elements compared to bulk HEAs. In recent years, novel HEA-NPs as electrocatalysts have been applied to redox reactions in batteries to figure out the problems that existed in conventional catalysts, such as scarcity and high prices of electrocatalysts based on precious metals (e.g., IrO_2 and RuO_2), low initial coulombic efficiency and fast capacity fading of batteries [2, 3]. Yao and co-workers introduced the carbothermal shock preparation of HEA-NPs, leading to the studies of nanoscale HEAs in the catalysis field [4]. Several encouraging synthetic strategies have been established to fabricate a range of HEA-NPs with excellent catalytic performance thanks to the endeavors of research teams worldwide. For example, Sharma et al. developed low-cost and effective Co-Fe-Ga-Ni-Zn HEA for oxygen evolution reaction (OER) catalysis, a vital part of rechargeable metal-air batteries [2]. Li et

al. reported a nanoporous Al-Cu-Ni-Pt-Mn HEA with ~20-30 at.% Pt loading, which not only exhibited exceptional oxygen reduction reaction (ORR) and electrochemical cycling durability but also realized less than 50 at.% Pt-based alloy catalysts [5]. Jin and colleagues have introduced a novel set of HEA nanowires that incorporate Al, Ni, Co, and Ru, in addition to utilizing one of the following elements as electrocatalysts: Mo, Cu, V, or Fe. These nanowires exhibit exceptional trifunctional capabilities by effectively catalyzing hydrogen evolution reaction (HER), OER and ORR [6]. Many of the latest developments toward HEA-NPs as electrocatalysts involved in synthesis, characterization, and properties in the electrocatalysis field will be covered in this review by collecting published articles. Besides, the obstacles and outlook in this particular subject will be provided.

2. Synthesis Strategies of HEA-NPs Materials

The preparation of multi-component HEA-NPs is a daunting task not only because of the difficulty in decreasing the size of HEAs to the nanoscale but also because of the trouble in uniformly mixing metal elements with vastly dissimilar physical and chemical properties such as miscibility, reduction possibility and melting point at the nanoscale. In recent years, a cascade of innovative preparation strategies has been reported to realize the nanostructured HEAs with metal composition, particle size, and phase structure precisely controlled.

2.1. Carbothermal Shock Strategy

PtPdRhRuCe HEA-NPs as an ammonia oxidation catalyst was prepared by Yao et al. through a carbothermal shock (CTS) strategy [4]. The metallic salt precursor compounds denoted as MClxHy (with M representing elements like Pt, Pd, Ni, Fe, Co, Au, Cu, or Sn), were mixed within a solution and subsequently applied as a coating onto oxygenated carbon nanofibers (CNFs) with good conductivity. The precursor-loaded samples underwent an immediate thermally shocking and cooling process under Ar protection with ~2000K temperature, ~55ms duration of shocks, and ~105K/s temperature ramping rate order achieved by an electrical pulse (Fig. 1a). Under such conditions, small liquid metallic droplets decomposed from the precursors were induced by the high temperature and subsequently crystallized into homogeneous HEA-NPs comprised of a maximum of eight immiscible metal elements. The synthesized HEA-NPs are uniformly distributed across the CNFs. The CTS parameters such as substrate, shock temperature, shock length, and ramp heating or cooling rates can be controlled to obtain the multi-component HEA-NPs with specific structures, phases and sizes.

To prove the practicability of this strategy, quinary PtPdRhRuCe HEA-NPs were synthesized as catalysts for ammonia oxidation (Fig. 1b), which showed ~100% ammonia (NH3) conversion and >99% NO_x (x=1, 2) selectivity at a comparatively modest operating temperature of 700°C (Fig. 1c). For comparison, the similar catalyst with phase-separated heterostructures synthesized by wet impregnation method generated only 18.7% output of NO_x at identical temperature. The majority of production was N_2, shown in Fig. 1d. In addition. The HEA-NPs showed remarkable catalytic durability; no degradation regarding catalytic activity or selectivity during ~30h of long-term operational period at 700°C (Fig. 1e). Therefore, the fabrication of HEA-NPs through the CTS method has the potential to serve as a universal approach for the production of catalysts that exhibit high activity, durability, and cost-effectiveness.

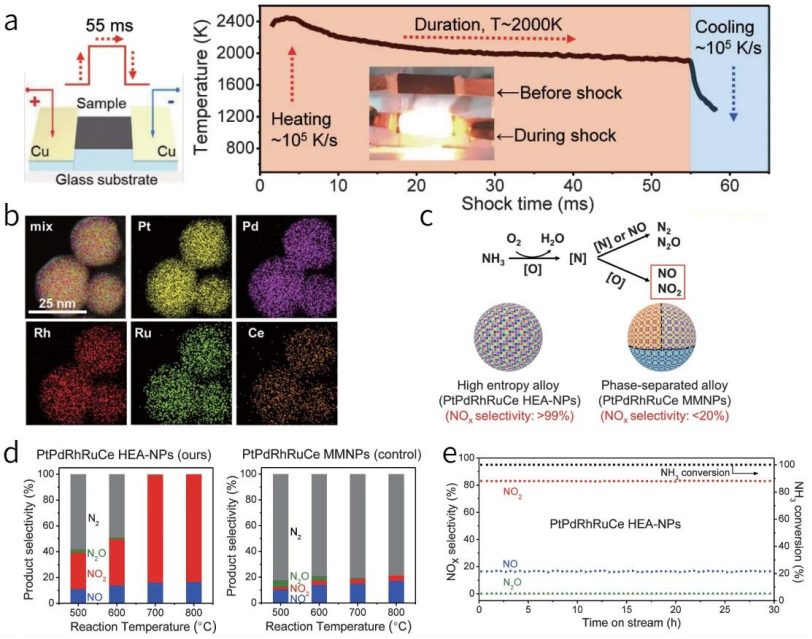

Figure 1. (a) Sample synthesis and temperature change over time regarding 55-ms thermal shock. (b) STEM elemental maps. (c) Reaction diagram for the differences of ammonia oxidation between PtPdRhRuCe HEA-NP and control sample. (d) Distribution of products and NH3 oxidation. (e) The catalytic efficiency changes over time at 700°C [4]

2.2. Low-Temperature Oil Phase Strategy

Since Ni, Fe, Co, and Cu are extremely abundant and easy to combine with Pt to form a solid solution, Li et al. selected these transition metallic elements with similar atomic size and lower formation heat to synthesize small PtNiFeCoCu HEA-NPs with diameter ~ 3.4nm through low-temperature oil phase method [7]. To prepare the PtNiFeCoCu HEA-NPs, $Pt(acac)_2$, $Ni(acac)_2$, $Fe(acac)_3$, $Co(acac)_3$, $Cu(acac)_2$, $Mo(CO)_6$, and glucose were mixed with trimethylammonium chloride and oleylamine while stirring at 400 rpm to produce a uniform solution, then the homogeneous mixture was heated to 220°C for 2h. Afterward, the carbon in ethanol was mixed with synthesized HEA-NPs in cyclohexane to obtain PtNiFeCoCu/C catalyst.

PtNiFeCoCu/C, an excellent redox bi-function electrocatalyst for methanol oxidation reaction (MOR) and HER, exhibited great stability and anti-CO toxicity properties in the alkaline medium. The multi-active sites on the suitable electronic surfaces of HEA-NPs are crucial in supplying quick area-to-area electron transfer toward oxidation and reduction reactions. It showed that PtNiFeCoCu/C catalyst has much lower conversion resistance, larger interfacial charge transfer rate, and more catalysis active sites than commercial Pt/C catalysts toward HER and MOR.

2.3. Precursor Fast Cooling and De-Alloying Strategy

Low Pt content senary AlNiCuPtPdAu HEA-NPs with ~2-3nm size and accurately regulated structure as catalysts of various reactions such as CO oxidation, HER, and ORR were prepared by Qiu et al. though precursor fast cooling and de-alloying strategy [8]. It is reported that the AlNiCuPtPdAu HEA-NPs exhibited highly improved stability under high temperatures (over 600°C) and great catalytic activity of CO oxidation with a naturally generated γ-Al_2O_3 thin oxide film. The HEA-NPs exhibited exceptional opposition towards coarsening at 200°C without the oxide layer. To prepare the HEA-NPs, pure metals were melted in an induction melting furnace with noble gas protection. The formed precursor alloys with compositions of $Al_{97.5}Ni_{0.5}Cu_{0.5}Pt_{0.5}Pd_{0.5}Au_{0.5}$ (at%) were then rotated to synthesize the alloy ribbons, which were ~2mm wide and ~20um thick. Then, the ultrafine nanoporous HEA (~3nm) with accurately controlled metal composition could be obtained by chemical de-alloying of the alloy ribbons in NaOH solution. The as-synthesized HEA-NPs were further etched in H_2SO_4 solution for 30 min to eliminate the oxide covering. Compared to

the Pt/C catalyst, the senary AlNiCuPtPdAu catalyst exhibited a higher current density and retained 92.5% of its original performance after undergoing 100,000 electrochemical cycles. The Pt mass-specific activity of HEA-NPs was ~5.5 times and ~10 times that of Pt/C toward HER and ORR, respectively.

2.4. Fast Moving Bed Pyrolysis Strategy

It is revealed that HEA-NPs dispersedly loaded on granular supports, including zeolite, Al_2O_3, and active carbon materials (carbon black and graphene oxide), could highly improve the surface energy and specific surface area relative to bulk HEAs. These immobilized HEA-NPs exhibited enhanced catalytic performance owing to adjustable size, shape, and stability. Gao and coworkers successfully synthesized HEA-NPs consisting of 10 immiscible metals (Co, Ni, Cu, Mn, Pd, Rh, Sn, Pt, Ir, and Au) with ultrasmall size ~2nm and face-centered crystal framework uniformly immobilizing on various supports via fast-moving bed pyrolysis (FMBP) [9] (Fig. 2a, d, e, f). FMBP method confirms that the mixed metal precursors could be pyrolyzed at once because of the rapid heating to 923K within 5s toward metal precursors. The obtained monomers are highly supersaturated, creating smaller nuclei clusters to produce homogeneous HEA-NP. By contrast, the conventional fixed bed pyrolysis (FBP) method can only prepare phase-separated alloys since the reduction of each metal precursor would occur sequentially based on their different reduction potentials. Different reduction potentials (Fig. 2b). Researchers also simulated the thermal transfer of precursors/graphene oxide (GO), it indicated that GO reached 923K in 5s (Fig. 2c). In terms of electrochemical water splitting, quinary FeCoPdIrPt HEA-NPs showed greater mass activity and lower overpotential of HER in comparison to Pt/C.

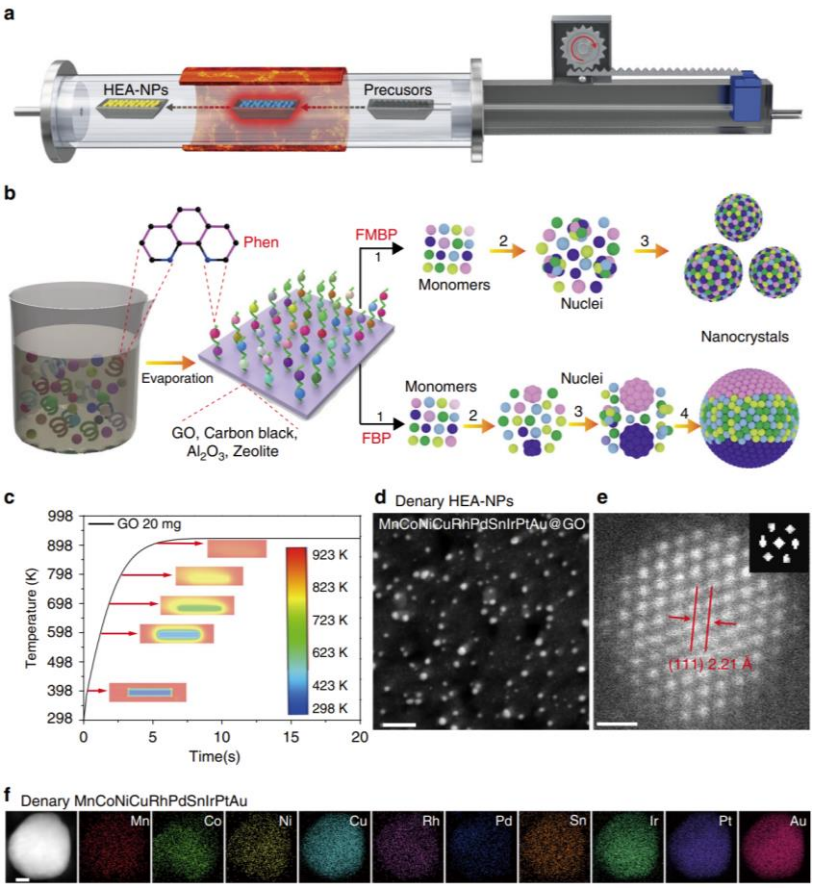

Figure 2. FMBP method for HEA-NPs preparation. (a) Graph of FMBP experiment setting. (b) Graphs of synthesis. (c) The evaluation of time to achieve 923K. d) HAADF-STEM images. (e) The HR-STEM image of MnCoNiCuRhPdSnIrPtAu HEA-NPs showing their fcc structure. (f) Elemental maps of HEA samples with equal atomic ratio [9]

3. Application of HEA-NPs in Electrocatalysis

3.1. Alkaline Seawater Splitting

Clean hydrogen production by water cracking has received increasing attention despite the high expense of noble metal-based electrocatalysts, the large amount of energy consumed and the need for fresh water. Electrocatalytic saltwater electrolysis can be an effective and cost-saving strategy to achieve hydrogen deposition due to the high ionic conductivity of superior saltwater solution. A kind of new HEA-NPs composed of Fe, Co, Mn, Ni, and Ru loaded on carbon nanotubes support (FeNiCoMnRu@CNT) was prepared by Zhang and coworkers through hydrothermal means (Fig. 3a), which exhibited superior OER and HER characters in overall alkaline seawater splitting (OWS) [10]. Carbon nanotubes' wire-like and finned structure is accumulated with separated pores, resulting in the uniform dispersion of HEA-NPs and easily connecting HEA electroactive sites to promote electron diffusion and transport.

When evaluating the HER performance, the FeNiCoMnRu@CNT attained a lowest overpotential of 50mV and a Tafel slope of 50mV dec^{-1} at 10mA cm^{-2}, which indicated the HER performance was much greater than other reported catalysts, such as NiCoP/NiCo-LDH@NF (213mV), 1D-Cu@Co-CoO/Rh (137mV), and CoP_x@FeOOH (117mV) with the same current densities in alkaline seawater. When examining OER activity, FeNiCoMnRu@CNT demonstrated the overpotential of 319mV, a Tafel slope of 56mV dec^{-1} at 10mA cm^{-2} and a charge transfer resistance of 0.6Ω, which also indicated the OER performance was much better than that of other catalysts. To evaluate the practical application of HEA-NPs, a prolonged OWS durability test of 30h was performed at a fixed power concentration of 10mA cm^{-2} (Fig. 3b). In Fig. 3c, no apparent attenuation could be observed over the 30h trial. FeNiCoMnRu@CNT achieved the voltage of 1.6V at j=10mA cm^{-2}, which was substantially greater compared to the constant potential of several recently described catalysts, such as $NiCo_2O_4$ (1.65V), NiSe/NF (1.63V), MoS_2-NiS_2/NGF (1.77V) and Ni-Co-P HNBs (1.62V) (Fig. 3d). For the hydrolysis system, the molar ratio between O_2 and H_2 produced was 1: 2 shown in Fig. 3f, g and the recorded gas volumes were perfectly consistent with expected values. Thus, this work paves the way for creating high-performance HEA electrocatalysts toward OER, HER, and OWS.

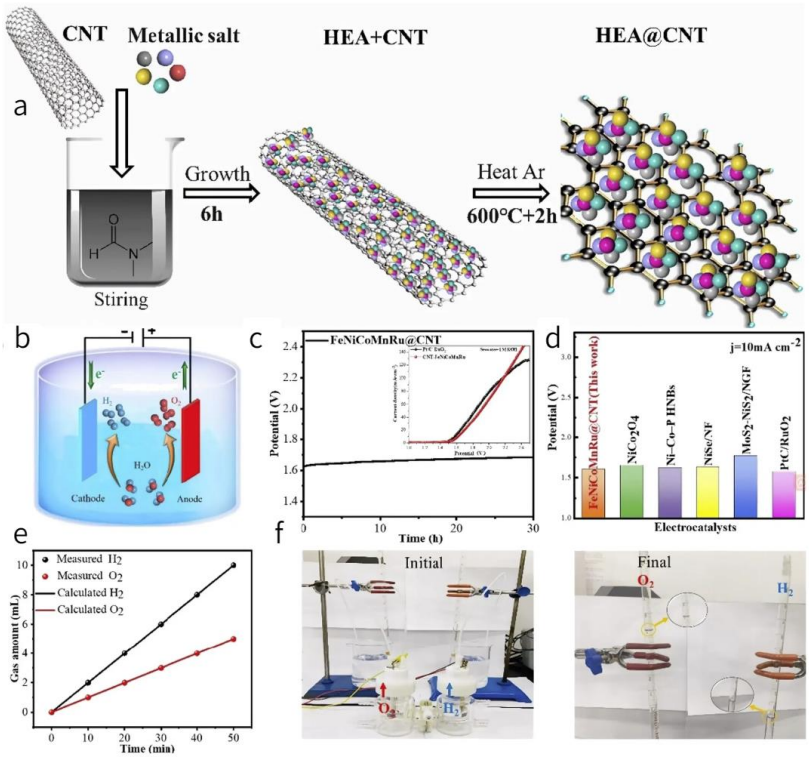

Figure 3. (a) Synthesis process of FeNiCoMnRu@CNT. (b) The schematic diagram for the water-splitting process. (c) The FeNiCoMnRu@CNT||FeNiCoMnRu@CNT electrodes split water well.

(d) The capacity of water splitting in alkaline seawater of various catalysts. (e) The volumes of O2 and H2 recorded by electrolyzer. (f) The quantity of gasses produced during water splitting [10]

3.2. Ammonia Decomposition

Catalyzing ammonia decomposition plays a vital role in many fields due to the potential use of NH_3 as a potentially effective liquid fuel for hydrogen storage. Ruthenium (Ru) shows the highest catalytic activity in the ammonia decomposition process, but the scarcity and high price of Ru limited extensive utilization. Then, a bimetallic Co-Mo alloy of earth-abundant metals is optimal for ammonia decomposition. However, the great miscibility gap significantly limits catalysis performance of Co-Mo (Fig. 4a). Herein, a novel category of HEA-NPs catalysts composed of earth-abundant Co, Mo, Fe, Ni, Cu for highly efficient ammonia decomposition was prepared by Xie and coworkers through carbothermal shock technique, and the miscibility restriction existed in Co-Mo alloys is overcome through manipulation of Co/Mo ratio in CoMoFeNiCu HEA-NPs [11].

The catalytic studies of HEA-Co_xMo_y NPs (~22nm in particle size) loaded on carbon nanofibers in a plug flow reactor under 5vol% NH_3 at 250-600°C were performed in comparison to Co-Mo alloy with 25/45 ratio (~20nm in particle size) and monometallic Ru (~2-3nm in particle size). The unloaded carbon nanofibers were determined to be inactive for NH_3. It showed that the conversion of NH_3 increased as the elevating temperature, and the conversion follows the order HEA-$Co_{25}Mo_{45}$ > HEA-$Co_{35}Mo_{35}$ > HEA-$Co_{15}Mo_{55}$ > HEA-$Co_{45}Mo_{25}$ > HEA-$Co_{55}Mo_{15}$ >Bimetallic Co-Mo between 300 and 500°C (Fig. 4b). The conversion reached saturation (100% conversion) at ~525°C for HEA-$Co_{25}Mo_{45}$ and at ~600°C for HEA-$Co_{55}Mo_{15}$. By contrast, Co-Mo alloy and Ru showed NH_3 conversions of only 46% and 73% at 600°C. When measuring the catalysis rate at 500°C among four catalysts (Fig. 4c). Apart from excellent activity, HEA-NPs $Co_{25}Mo_{45}Fe_{10}Ni_{10}Cu_{10}$ exhibited superior durability at 500°C for ~50h continuous operation with minimal attenuation (Fig. 4d).

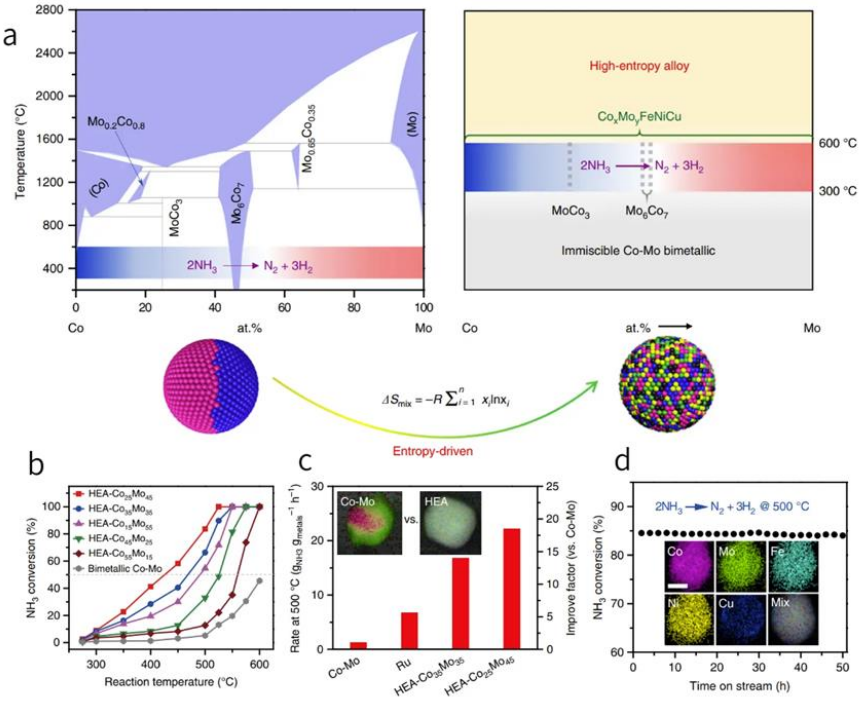

Figure 4. (a) The miscibility restriction of Co-Mo alloy overcomed by HEA catalyst. (b) Depending on the reaction temperature, NH3 conversions among various HEA-CoxMoy NPs and Co-Mo alloys with a 25/45 ratio. (c) A reaction rate comparison was recorded among HEA-CoxMoy, Ru, and Co-Mo at 500°C. (d) A durability test of the HEA-Co25Mo45 catalyst was conducted at 500°C [11]

4. Application of HEA-NPs in Redox Chemical Batteries

4.1. Lithium Sulfur Battery

In lithium-sulfur batteries, the initial S_8 obtains $16e^-$ and goes through solid-liquid-solid phase conversion to generate Li_2S, which enables Li-S batteries to hold a large specific capacity and theoretical energy density features [3]. However, during many multielectron and multiphase cathodic transitions of lithium polysulfides (LiPSs), the intermediates could readily diffuse between electrodes, and the Li_2S precipitation could encounter a large energy barrier (Fig. 5a), leading to the problems of reduced capacity, increased polarization, and low energy use. Xu and coworkers fabricated HEA-NPs comprised of Fe, Co, Ni, Mn, and Zn by carbothermal shock breakup of multimetal-MOF-74 as the catalyst for LiPSs redox reactions, which showed ~7nm size and consistent dispersion on carbon substrate.

Specifically, Zn serves as an electron storage site; Mn acts as the site of electron consumption, and other metals benefit the multielectron reactions by generating more continuous charge regulation. As Fig. 5b depicted, the HEA-NPs play a key role in decreasing polarization and energy loss not only by exhibiting high LiPS affinity, enhancing the activity of LiPSs close to the cathode, and decreasing the concentration polarization, but also by speeding up subsequent redox processes to suppress the activation polarization.

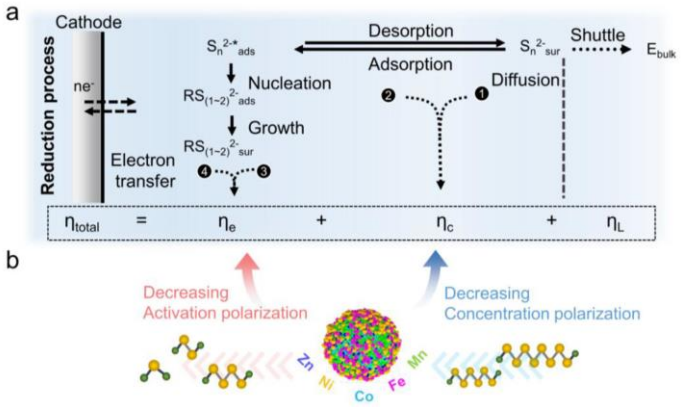

Figure 5. (a) LiPS's reduction mechanism and polarization characters. (b) A graph illustrating HEA-NPs can lower polarization in two ways [3]

4.2. Rechargeable Zn-Air Battery

Rechargeable zinc-air batteries depend heavily on active ORR catalysts during the discharge and active OER catalysts during the charging. However, noble metals are crucial in high-performance heterogeneous catalysis. For example, Pt-based catalysts show excellent performance toward ORR and HER processes; materials based on Ru and Ir are widely recognized as the greatest catalysts toward the OER process. Therefore, decreasing the application of such precious metals while improving the expected catalytic effect has been challenging. Jin et al. synthesized a series of HEA nanowires Al-Ni-Co-Ru-X (X represents Fe, Cu, V, Mo) through a straightforward de-alloying process, which can not only largely decrease the contents of precious metals but also greatly improve the flexibility of electronic structures appropriate for outstanding catalytic performance of HER, OER and ORR [6]. Al phase was eliminated in the de-alloying procedure, and Al-Ni-Co-Ru-X nanowires naturally formed multi-component surface spinel oxides (HEA/HEO nanowires). Through adjusting metal X, it showed that the AlNiCoRuMo HEA/HEO nanowires with diameters of 20-100nm (Fig. 6a, b) could be employed as the greatest trifunctional ORR, HER, and OER catalysts.

The AlNiCoRuMo air electrode was then integrated into a Zinc-air battery (Fig. 6c); as a comparison, a battery based on Pt/C-IrO_2 was constructed. The AlNiCoRuMo material displayed a voltage difference (ΔE) of 0.61V between the OER and half-wave potential for ORR at 10 mA cm^{-2}. This value was notably lower than the voltage difference of Pt/C-IrO_2 (ΔE=0.68V), indicating the

superior behavior of the Zn-air battery. Consequently, the battery based on AlNiCoRuMo demonstrated a larger open-circuit voltage of 1.48 V, increased energy density of 851.3Wh kg_{Zn}^{-1} at 20mA cm^{-2} (as shown in Fig. 6d), and a greater power density of 146.5 mW cm^{-2} (Fig. 6e) by comparison with the battery based on Pt/C-IrO. Additionally, the AlNiCoRuMo-based battery exhibited remarkable durability, maintaining a consistent voltage difference of approximately ~0.75V. when treated with continuous charging/discharging at 2mA cm^{-2} for more than 500h (Fig. 6f), illustrating the excellent durability and potential practical applications. When the current density was reset to 2mA cm^{-2} after prolonged discharge/charge cycles, the battery property could return to the initial state (Fig. 6g), demonstrating that the HEA/HEO electrocatalyst did not degrade. As a result, the multi-component AlNiCoRuMo HEA/HEO nanowires exhibited improved activities and reduced noble metal content for various applications.

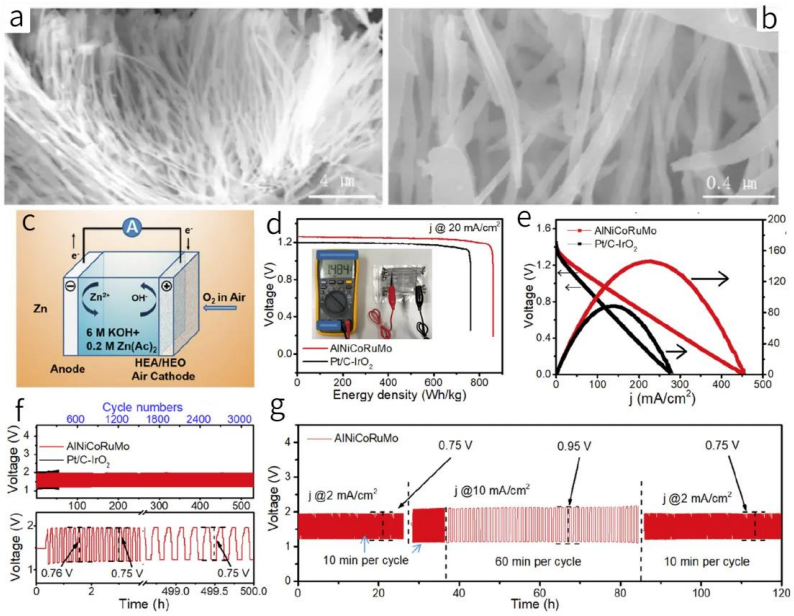

Figure 6. (a, b) SEM images of quinary AlNiCoRuMo nanowires. (c) Graph of a zinc-air battery. (d) Two different discharge curves. (e) Power densities of the batteries based on AlNiCoRuMo and Pt/C−IrO2. (f) Behaviors of two different zinc-air batteries under continuous charge/discharge cycling. (g) Cycling results in different discharge/charge periods [6].

5. Conclusion

Recently, HEA nanostructures have exhibited exceptional properties as heterogeneous catalysts because of their extensive chemical complexity and flexibility. On the basis of HEAs, “high-entropy” theory has been expanded to a range of high-entropy compounds, including high-entropy oxides (HEOs), borides (HEBs), silicides (HESs) and nitrides (HENs), and so on. The HEA solid solution that is configurationally disordered and entropy-stabilized significantly reduces the noble metal content of catalysts and shows optimal stability in a range of long-term reactions at a high temperature. The performance of many HEA-NPs can surpass the commercial catalysts such as Pt/C or Ir/C for various electrocatalytic processes, which have attracted intensive research in the electrocatalysis field.

Even though the HEA-NPs have shown great potential to be a class of excellent catalysts, several elementary and practical issues still pose significant challenges to HEA-NPs. 1) Although various well-established synthetic technologies have been created experimentally, advanced scale-up and low energy consumption strategies with simple and low-cost equipment suitable for industry fields need to be developed. 2) The correlation between structure and catalytic activity in HEAs still needs further identification. Because of HEAs' complex surface and internal structure, active sites' recognition and dynamic evolution behavior in HEA electrocatalysts remain ambiguous. 3) The most active HEA-NPs among many elemental combinations must be precisely identified and selected for various

reactions through high-throughput characterization of compositions and catalytic performance. 4) Advanced machine learning and big data-assisted research are needed to guide the preparation of novel HEA-NPs with more catalytically active sites. A better identification of the composition and catalysis mechanism of HEA-NPs can also be obtained through this.

References

[1] Yeh Jien-Wei, Chen Swe-Kai and Lin Su-Jien, et al. Nanostructured high-entropy alloys with multiple principal elements: novel alloy design concepts and outcomes. Advanced Engineering Materials, 2004, 6 (5): 273-349.

[2] Sharma Lalita, Katiyar Nirmal Kumar and Parui Arko, et al. Low-cost high entropy alloy (HEA) for high-efficiency oxygen evolution reaction (OER). Nano Research, 2022, 15 (6): 4799-4806.

[3] Xu Hongfei, Hu Riming and Zhang Yongzheng, et al. Nano high-entropy alloy with strong affinity driving fast polysulfide conversion towards stable lithium sulfur batteries. Energy Storage Materials, 2021, 43: 212–220.

[4] Yao Yonggang, Huang Zhennan and Xie Pengfei, et al. Carbothermal shock synthesis of high-entropy-alloy nanoparticles. Science, 2018 (359): 1489-1494.

[5] Li Shiyin, Tang Xiaowei and Jia Henglei, et al. Nanoporous high-entropy alloys with low Pt loadings for high performance electrochemical oxygen reduction. Journal of Catalysis, 2023, 383: 164-171.

[6] Jin Zeyu, Lyu Juan and Zhao Yi-Lu, et al. Rugged high-entropy alloy nanowires with in situ formed surface spinel oxide as highly stable electrocatalyst in Zn−air batteries. ACS Materials Lett. 2020, 2: 1698−1706.

[7] Li Hongdong, Han Yi and Zhao Huan, et al. Fast site-to-site electron transfer of high-entropy alloy nanocatalyst driving redox electrocatalysis. Nat Commun, 2020, 11: 5437.

[8] Qiu Hua-Jun, Fang Gang and Yuren Wen, et al. Nanoporous high-entropy alloys for highly stable and efficient catalysts. J. Mater. Chem. A, 2019, 7: 6499.

[9] Gao Shaojie, Hao Shaoyun and Huang Zhennan, et al. Synthesis of high-entropy alloy nanoparticles on supports by the fast moving bed pyrolysis. Nat Commun 2020, 11: 2016.

[10] Zhang Quan, Lian Kang and Liu Qian, et al. High entropy alloy nanoparticles as efficient catalysts for alkaline overall seawater splitting and Zn-air batteries. Journal of Colloid and Interface Science 2023, 646: 844–854.

[11] Xie Pengfei, Yao Yonggang and Huang Zhennan, et al. Highly efficient decomposition of ammonia using high-entropy alloy catalysts. Nat Commun 2019, 10: 4011.